DEPENDENCE OF PEIERLS TRANSITION ON CARRIER CONCENTRATION IN ORGANIC CRYSTALS OF TTT_2I_3 IN THE 3D APPROXIMATION

S. Andronic and A. Casian

Technical University of Moldova, Stefan cel Mare Avenue 168, Chisinau, MD-2004 Republic of Moldova
E-mail: andronic_silvia@yahoo.com

(Received November 19, 2018)

Abstract

The dependence of the Peierls structural transition on carrier concentration in quasi-one-dimensional (Q1D) organic crystals of TTT_2I_3 is studied in the 3D approximation. A more complete physical model that considers simultaneously two most important electron–phonon interactions is used. The first interaction is similar to that of deformation potential, while the second one is of the polaron type. The dynamical interaction of carriers with defects is also taken into account. An analytic expression for the phonon Green function is obtained in the random phase approximation. A renormalized phonon spectrum is determined for different values of dimensionless Fermi momentum k_F. In all cases, the Peierls critical temperature is determined.

1. Introduction

Quasi-one-dimensional organic crystals of tetrathiotetracene iodide (TTT_2I_3) exhibit promising thermoelectric properties. These materials were synthesized independently and nearly simultaneously [1–4] with the aim to find superconductivity in a low-dimensional conductor. At the same time, these crystals show a metal–dielectric transition with decreasing temperature.

Tetrathiotetracene iodide crystals are composed of segregate chains of TTT and iodine. Tetrathiotetracene iodide is a charge-transfer compound. The lattice constants are a = 18.40 Å, b = 4.96 Å, and c =18.32 Å, which are indicative of a pronounced crystal quasi-one-dimensionality. The highly conducting direction is that along ***b***. The compound is of mixed valence. Two molecules of TTT give one electron to the iodine chain composed of I_3^- ions, which play the role of acceptors. However, the crystals admit a nonstoichiometric composition with a surplus or deficiency of iodine. Therefore, the metal–dielectric transition takes place at different carrier concentrations.

The Peierls transition was studied by many authors (see [5–7] and references therein). Earlier, it was shown for a $TTT_2I_{3.1}$ crystal that the transition is of Peierls type.

Previously [8], the Peierls transition in TTT_2I_3 crystals was analyzed in the 2D approximation. It was found that the Peierls transition begins at T ~ 35 K in TTT chains and considerably reduces the electrical conductivity. Due to the interchain interaction, the transition is completed at T ~ 19 K.

A 3D physical crystal model was studied in [9]. A $TTT_2I_{3.1}$crystal was analyzed. In this case, dimensionless Fermi momentum $k_F = 0.517\pi/2$. The transition begins at T ~ 35 K in TTT chains. Due to the interchain interaction, the transition is completed at T ~ 9.8 K. It was observed

in experiments that the electrical conductivity has a maximum at 35 K and achieves zero at $T \sim 10$ K. It was shown that the hole–phonon interaction and the interactions with structural defects diminish the renormalized phonon spectrum $\Omega(q_x)$ and reduce the sound velocity in a wide temperature range.

In this paper, we study the behavior of the Peierls transition in TTT_2I_3 crystals in the 3D approximation for different k_F values that is determined by variations in the carrier concentration. Defect scattering is also considered. Peierls critical temperature T_p is determined for different values of dimensionless Fermi momentum $k_F - \delta$, where δ is the variation in Fermi momentum k_F due to a decrease in the carrier concentration. The results obtained in the 3D physical model are analyzed and commented in detail.

2. Three-Dimensional Physical Model of the Crystal

The physical model of the crystal was described in more detail in [8]. The Hamiltonian of the 3D crystal model in the tight binding and nearest neighbor approximations has the form

$$H = \sum_{\boldsymbol{k}} \varepsilon(\boldsymbol{k}) a_{\boldsymbol{k}}^{+} a_{\boldsymbol{k}} + \sum_{\boldsymbol{q}} \hbar\omega_{\boldsymbol{q}} b_{\boldsymbol{q}}^{+} b_{\boldsymbol{q}} + \sum_{\boldsymbol{k},\boldsymbol{q}} A(\boldsymbol{k},\boldsymbol{q}) a_{\boldsymbol{k}}^{+} a_{\boldsymbol{k}+\boldsymbol{q}} (b_{\boldsymbol{q}} + b_{-\boldsymbol{q}}^{+}) \tag{1}$$

where the first term is the energy operator of free holes in the periodic field of the lattice. The second term is the energy operator of longitudinal acoustic phonons; the third term represents the hole–phonon interactions; and $a_{\boldsymbol{k}}^{+}$, $a_{\boldsymbol{k}}$ are the creation and annihilation operators of the hole with a 3D quasi-wave vector $\boldsymbol{k}$ and projections (k_x, k_y, k_z). The energy of the hole $\varepsilon(\boldsymbol{k})$, measured from the band top is presented in the form

$$\varepsilon(\boldsymbol{k}) = -2w_1(1-\cos k_x b) - 2w_2(1-\cos k_y a) - 2w_3(1-\cos k_z c) \tag{2}$$

where w_1, w_2 and w_3 are the transfer energies of a hole from one molecule to another along the chain (x direction) and perpendicular to it (y and z directions). In Eq. (1), $b_{\boldsymbol{q}}^{+}$, $b_{\boldsymbol{q}}$ are the creation and annihilation operators of an acoustic phonon with 3D wave vector $\boldsymbol{q}$ and frequency $\omega_{\boldsymbol{q}}$. The Peierls transition occurs at low temperatures. In this case, the interaction of electrons with optical phonons can be neglected. It was shown in [10] that the spectrum of acoustic phonons of a simple one-dimensional chain is described by

$$\omega_{\boldsymbol{q}}^2 = \omega_1^2 \sin^2(q_x b/2) + \omega_2^2 \sin^2(q_y a/2) + \omega_3^2 \sin^2(q_z c/2) \tag{3}$$

where ω_1, ω_2, and ω_3 are the limit frequencies in the x, y, and z directions. Two most important electron–phonon interaction mechanisms are considered: one of the deformation potential type and the other of the polaron type. The coupling constants of the first interaction are proportional to derivatives w_1', w_2' and w_3' of w_1, w_2, and w_3 with respect to the intermolecular distances. The coupling constant of the second interaction is proportional to the average polarizability of the molecule α_0. This interaction is important for crystals composed of large molecules, such as TTT, so as α_0 is roughly proportional to the molecule volume.

The square module of matrix element $A(\boldsymbol{k},\boldsymbol{q})$ from Eq. (1) can be written in the form

$$\begin{aligned}\left|A(\boldsymbol{k},\boldsymbol{q})\right|^2 = 2\hbar w_1'^2/(NM\omega_{\boldsymbol{q}})\times\{[\sin(k_x b)-\sin(k_x-q_x,b)-\gamma_1\sin(q_x b)]^2+\\ d_1^2[\sin(k_y a)-\sin(k_y-q_y,a)-\gamma_2\sin(q_y a)]^2+d_2^2[\sin(k_z c)-\sin(k_z-q_z,c)-\gamma_3\sin(q_z c)]^2\}.\end{aligned} \tag{4}$$

Here, M is the mass of the molecule; N is the number of molecules in the basic region of the crystal; $d_1 = w_2/ w_1 = w_2'/w_1'$; $d_2 = w_3/ w_1 = w_3'/w_1'$; parameters γ_1, γ_2, and γ_3 describe the ratio of amplitudes of the polaron-type interaction to the deformation potential one in the *x*, *y*, and *z* directions:

$$\gamma_1 = 2e^2\alpha_0/b^5 w_1',\ \gamma_2 = 2e^2\alpha_0/a^5 w_2',\ \gamma_3 = 2e^2\alpha_0/c^5 w_3'\ . \tag{5}$$

In the reported results of experimentally measured longitudinal electrical conductivity of TTT_2I_3 crystals as a function of temperature, a sharp decrease in electrical conductivity for temperatures lower than $T_{\max}$ = 35 K is observed [2]. Analysis shows that the Hamiltonian from Eq. (1) can not explain this behavior of the electrical conductivity. In addition, it is necessary to take into account the dynamical interaction of carriers with defects. The static interaction will contribute to the renormalization of the hole spectrum. The defects in TTT_2I_3 crystals are formed due to different coefficients of dilatation of the TTT and iodine chains. The Hamiltonian of this interaction H_{def} is presented in the form

$$H_{def} = \sum_{\boldsymbol{k},\boldsymbol{q}}\sum_{n=1}^{N_d} B(q_x)\exp(-iq_x x_n)a_{\boldsymbol{k}}^{+}a_{\boldsymbol{k}-\boldsymbol{q}}(b_{\boldsymbol{q}}+b_{\boldsymbol{q}}^{-})\ . \tag{6}$$

Here, $B(q_x)$ is the matrix element of a hole interaction with a defect; it is presented as follows:

$$B(q_x) = \sqrt{\hbar/(2NM\omega_q)}\cdot I(q_x), \tag{7}$$

where $I(q_x)$ is the Fourier transformation of the derivative with respect to the intermolecular distance from the energy of interaction of a carrier with a defect, x_n numbers the defects, which are considered linear along the *x*-direction of the TTT chains and distributed randomly:

$$I(q_x) = D(\sin(bq_x))^2, \tag{8}$$

where constant D = 1.03; it determines the intensity of the hole interaction with a defect.

The renormalized phonon spectrum, $\Omega(\boldsymbol{q})$ is determined by the pole of the Green function and obtained from the transcendent dispersion equation

$$\Omega(\boldsymbol{q}) = \omega_{\boldsymbol{q}}[1-\overline{\Pi}(\boldsymbol{q},\Omega)]^{1/2} \tag{9}$$

where the principal value of the dimensionless polarization operator takes the form

$$\operatorname{Re}\overline{\Pi}(\boldsymbol{q},\Omega) = -\frac{4}{\hbar\omega_q}\sum_{\boldsymbol{k}}\frac{\left[\left|A(\boldsymbol{k},-\boldsymbol{q})\right|^2+\left|B(q_x)\right|^2\right](n_k-n_{k+q})}{\varepsilon(\boldsymbol{k})-\varepsilon(\boldsymbol{k}+\boldsymbol{q})+\hbar\Omega} \tag{10}$$

Here, n_k is the Fermi distribution function. Equation (9) can be solved only numerically.

3. Results and Discussion

Numerical simulations for the 3D physical model of the crystal are performed for the following parameters [11]: $M = 6.5 \times 10^5\ m_e$ (m_e is the mass of the free electron), $w_1 = 0.16$ eV, $w_1' = 0.26$ eV·Å^{-1}, $d_1 = 0.015$, $d_2 = 0.015$, $\gamma_1 = 1.7$, γ_2 and γ_3 are determined from the following relationships: $\gamma_2 = \gamma_1 b^5 / a^5 d_1$ and $\gamma_3 = \gamma_1 b^5 / c^5 d_2$. The sound velocity along the TTT chains was estimated by comparison of the calculated results for the electrical conductivity of TTT_2I_3 crystals with the reported ones [2], $v_{s1} = 1.5 \times 10^5$ cm/s. For v_{s2} and v_{s3} in transversal directions (in the *a* direction and the *c* direction), we took 1.35×10^5 cm/s and 1.3×10^5 cm/s, respectively.

Figures 1–4 show dependences of renormalized phonon frequencies $\Omega(q_x)$ as a function of q_x for different temperatures and different of q_y and q_z values. The same figures show dependences for initial phonon frequency $\omega(q_x)$. It is evident that the $\Omega(q_x)$ values are diminished compared with those of $\omega(q_x)$ in the absence of the hole–phonon interaction. This means that the hole–phonon interaction and structural defects diminish the values of lattice elastic constants. In addition, one can observe that, with a decrease in temperature *T*, the curves change their form and a minimum appears in the $\Omega(q_x)$ dependences. This minimum becomes more pronounced at lower temperatures.

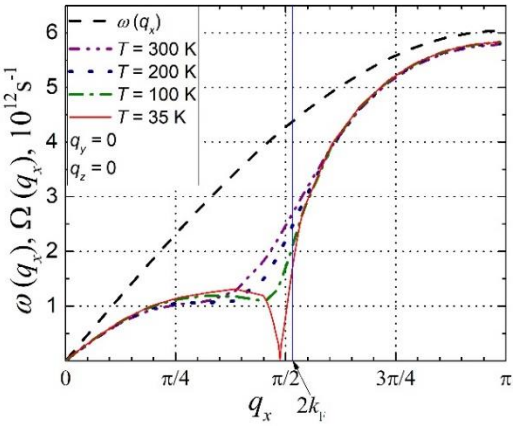

Fig. 1. Renormalized phonon spectrum $\Omega(q_x)$ for $\gamma_1 = 1.7$ and different temperatures. The dashed line is for the spectrum of free phonons. $k_F = 0.517\pi/2$.

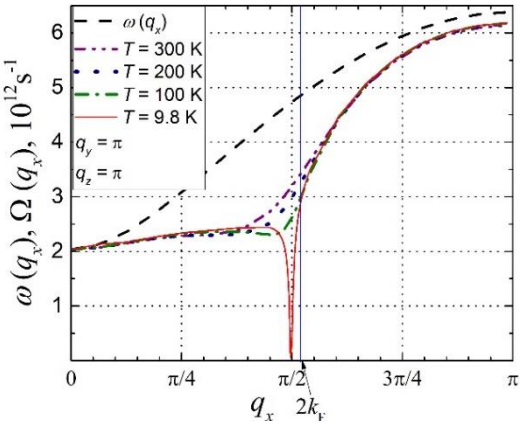

Fig. 2. Renormalized phonon spectrum $\Omega(q_x)$ for $\gamma_1 = 1.7$ and different temperatures. The dashed line is for the spectrum of free phonons. $k_F = 0.517\pi/2$.

Figures 1 and 2 were analyzed in detail in [9]. Figure 1 shows the case where $q_y = 0$ and $q_z = 0$ and dimensionless Fermi momentum $k_F = 0.517\pi/2$. In this case, the interaction between the TTT chains is neglected. The Peierls transition begins at $T = 35$ K. At this temperature, the electrical conductivity is significantly diminished, so as a gap in the carrier spectrum is fully opened just above the Fermi energy. In addition, it is evident that the slope of $\Omega(q_x)$ at low $\Omega(q_x)$ is diminished compared with that of $\omega(q_x)$. This means that the hole–phonon interaction and structural defects have reduced also the sound velocity in a wide temperature range. If the interaction between transversal chains is taken into account ($q_y \neq 0$ and $q_z \neq 0$), the temperature at $\Omega(q_x) = 0$ is diminished. This case is shown in Fig. 2 ($q_y = \pi$ and $q_z = \pi$) and $k_F = 0.517\pi/2$. It is

evident from the graph that the transition is completed at T ~ 9.8 K. According to [4], the electrical conductivity significantly decreases and achieves zero at T ~ 10 K. Thus, our calculations show that the transition is of the Peierls type and completed at this temperature.

Figure 3 shows the case where the Fermi momentum decreases and has a value of $k_F = (0.517\pi/2) - 0.018$. In Fig.3, the case where $q_y = 0$ and $q_z = 0$ is presented. It is evident that the Peierls transition begins at $T = 57$ K.

Figure 4 shows the case where the interaction between the TTT chains is taken into account ($q_y = \pi$ and $q_z = \pi$) and the Fermi momentum has the same value of $k_F = (0.517\pi/2) - 0.018$. It is evident that, at $\Omega(q_x) = 0$, the temperature decreases considerably, namely, to $T = 14$ K.

It was found that, with a decrease in the carrier concentration, T_p increases. For $k_F = 0.517\pi/2$, the transition begins at T ~ 35 K and is completed at T ~ 9.8 K. For $k_F = (0.517\pi/2) - 0.018$, the transition begins at T ~ 57 K at $q_y = 0$ and $q_z = 0$ and is completed at T ~ 14 K at $q_y = \pi$ and $q_z = \pi$.

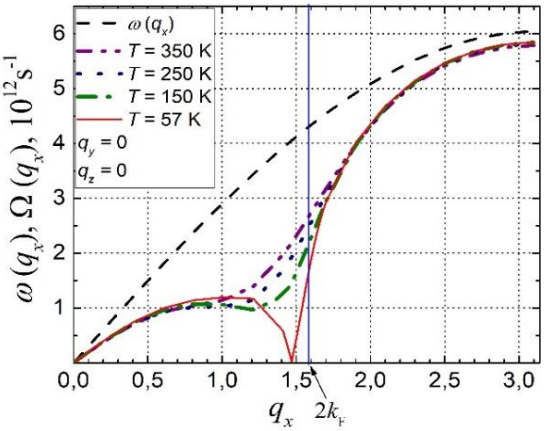

Fig. 3. Renormalized phonon spectrum $\Omega(q_x)$ for $\gamma_1 = 1.7$ and different temperatures. The dashed line is for the spectrum of free phonons. $k_F=(0.517\ \pi/2) - 0.018$.

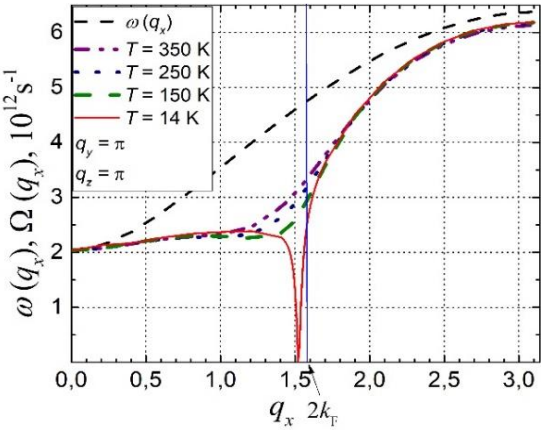

Fig. 4. Renormalized phonon spectrum $\Omega(q_x)$ for $\gamma_1 = 1.7$ and different temperatures. The dashed line is for the spectrum of free phonons. $k_F=(0.517\ \pi/2) - 0.018$.

4. Conclusions

The dependence of the Peierls structural transition on carrier concentration in quasi-one-dimensional (Q1D) organic crystals of TTT_2I_3 is studied in the 3D approximation. A more complete crystal model is used; it takes into account two most important hole–phonon interactions. The interaction of holes with structural defects in the direction of the TTT chains is taken into account too. An analytical expression for the polarization operator is derived in the random phase approximation. The method of retarded temperature dependent Green function is applied. The numerical calculations for renormalized phonon spectrum $\Omega(q_x)$ for different temperatures are presented in two cases: (i) at $k_F = 0.517\pi/2$ and (ii) at a varying carrier concentration and $k_F = 0.517\pi/2 - \delta$, where δ is the variation in Fermi momentum k_F, which is determined by the decrease in the carrier concentration. It is found that, at $k_F = 0.517\pi/2$, the Peierls transition begins at T ~ 35 K in the TTT chains and considerably decreases the electrical

conductivity. Due to the interchain interaction, the transition is completed at $T \sim 9.8$ K. It is shown that the transition is of the Peierls type, so as at $T \sim 10$ K the electrical conductivity achieves zero. The hole–phonon interaction and the interactions with structural defects also diminish $\Omega(q_x)$ and reduce the sound velocity in a wide temperature range. It is observed that, with a decrease in carrier concentration, the Peierls critical temperature increases.

Acknowledgments. The authors express gratitude to the support of the scientific program of the Academy of Sciences of Moldova under project no. 14.02.116F.

References

[1] I.I. Buravov, G.I. Zvereva, V.F. Kaminskii, et.al., Chem. Commun. 18, 720 (1976).
[2] V.F. Kaminskii, M.l. Kidekel', Lyubovskii, et. al., Phys. Status Solidi A 44, 77 (1977).
[3] B. Hilti and C.W. Mayer, Helv. Chim. Acta 61, 501 (1978).
[4] L.G. Isset and E.A. Perz-Albuerene, Sol. State Comm., 21, 433 (1977).
[5] L. N. Bulaevskii, Usp. Fiz. Nauk 115, 263 (1975).
[6] M. Hohenadler, H. Fehske, and F.F. Assaad, Phys. Rev. B 83, 115105 (2011).
[7] V. Solovyeva et al., J. Phys. D: Appl. Phys. 44, 385301 (2011).
[8] S. Andronic and A. Casian, Adv. Mater. Phys. Chem. 7, 212 (2017).
[9] S. Andronic, I. Balmus, and A. Casian, 9th Int. Conf. on Microelectronics and Computer Science, Chisinau, Republic of Moldova, October, 19–21, 2017.
[10] A. Graja, Low-dimensional organic conductors, Singapore, Word Scientific, 1989.
[11] A. Casian and I. Sanduleac, J. Electron. Mater. 43, 3740 (2014).